*Bull. Pharm. Sci., Assiut University, Vol. 47, Issue 1, 2024, pp. 499-517.*

*Bulletin of Pharmaceutical Sciences*
**Assiut University**
*Website: http://bpsa.journals.ekb.eg/*

BULL. PHARM. SCI. Assiut Univ.

# BIOSYNTHESIS OF ZINC OXIDE NANOPARTICLES USING *ALOE VERA* LEAVES EXTRACT AND THEIR ANTIBACTERIAL IMPACT

Magdy A. Abu-Gharbia, Jehan M. Salem, Gehad Al-Arabi*

*Botany and Microbiology Department, Faculty of Science, Sohag University, 82524 Sohag, Egypt*

*Zinc oxide nanoparticles (ZnO NPs) have gained a huge interest as a promising therapeutic alternative for antibiotics. In this study, the biosynthesis of ZnO NPs was performed using Aloe vera leaves extract in a remarkably simple approach. The biosynthesized ZnO NPs were detected by UV-Vis spectrophotometer at wavelength of 383 nm. The x-ray diffraction analysis indicated the hexagonal wurtzite of ZnO NPs with a median crystallite size of 16.7 nm. Transmission and scanning electron microscopy exhibited the hexagonal shape of ZnO NPs with a median particle size of ~ 20 nm. Fourier transform infrared analysis showed the mutual presence of phenolic compounds in Aloe vera leaves extract and ZnO NPs which reflected their principle role in the bio-reduction. From our perspective, the optimum conditions for the biosynthesis of ZnO NPs with smaller sizes included zinc nitrate concentration of 0.01-0.03M, Aloe vera extract concentration of 50%, pH=8, and 25-40 ℃. The antibacterial impact of ZnO NPs was confirmed against both Gram-negative and Gram-positive bacterial isolates. Values of minimum inhibitory concentration (MIC) of ZnO NPs varied to be 2-4.1 mg/ml and 8.2-11 mg/ml for Gram-negative and Gram-positive bacterial isolates, respectively. Furthermore, ZnO NPs exhibited bactericidal impact on all tested bacterial isolates with minimum bactericidal concentration (MBC) of 2.1-4.7 mg/ml and 8.2-11.4 mg/ml for Gram-negative and Gram-positive bacterial isolates, respectively*

***Keywords:*** *Green synthesis, Aloe vera, ZnO NPs, phenolic compounds, bactericidal effect*

## INTRODUCTION

Nanotechnology is an arising area of research that deals with nano-scaled particles with dimensions mainly less than 100 nm[1]. Nanoscale dimensions provide the nanoparticle (NP) with a large surface area to volume ratio and thus highly unique properties including optical, electronic, and medicinal properties. Therefore, NPs play a vital role in several fields of application such as cosmetics, healthcare, agricultural, and pharmaceuticals[1]. Recently, NPs have vastly emerged as an antibacterial agents and they have been proved to be useful particularly for inhibiting drug-resistant bacteria[2,3]. The NPs can exhibit their bacteriostatic and bactericidal effects by disrupting the bacterial cell membrane[60-62]. Due to its large surface area to volume ratio, the NP can accommodate a large number of ligands for better targeting of pathogenic microbes[4].

Various methods can be used for the synthesis of NPs such as chemical, physical, and biological methods. Synthesis of NPs by chemical and physical methods releases some toxic byproducts in the manufacturing process. These toxic chemicals are extremely hazardous to the environment and may cause health related problems[5]. Consequently, the biological methods have been adopted. Biological synthesis, also termed green synthesis, aims to the use of bacteria, fungi, algae, and plant parts to synthesize NPs. This technique helps to reduce the toxicity of metal and also does not produce toxic by-products[6].

Researchers have shown a huge interest towards the biosynthesis of NPs via the plant extracts[7]. Plant-mediated synthesis of NPs

*Received : 28/9/2023 & Accepted : 26/11/2023*

*Corresponding author: Gehad Al-Arabi, E-mail: gehad2014119@science.sohag.edu.eg or alarabygehad94@gmail.com

exceeds other methods by several advantages as it is a reliable method, cost effective, simple, eco-friendly, reduced in toxic and hazardous products[8,9], and importantly, it needs no additional chemicals[10]. The green process takes truly little time, less energy, and does not involve costly equipment and precursors[11,12]. In addition, NPs synthesized via the plant-mediated approaches are highly pure, stable, varied in shape and size and produced in large scale. Extracts of plant parts (e.g., roots, leaves, stems, fruits, or seeds) utilized for the NPs synthesis are comprised of phytochemical biomolecules which are responsible for the bio-reduction process[13]. Bio-reduction embraces reducing metal ion to zero valence metal nanoparticle with the aid of these phytochemicals that can also function as stabilizing agents[14]. In particular, *Aloe vera* has been known for centuries with its curative and therapeutic properties in addition to the presence of medicinally active constituents like tannins, saponins, phlobbasstannis, steroid, terpenoids, flavonoids, and glycosides[15].

Among various metal and metal oxide NPs reported to have medicinal properties, Zinc oxide nanoparticles (ZnO NPs) have gained a unique attention as they are convincible to be used for the biological applications[19]. ZnO NPs are widely used in cosmetics like sunscreen lotions due to their UV filtering properties. They provide high protection against the harmful effects of UV-A and UV-B such as photoaging, carcinogenic, and immunosuppressant impacts[16]. In addition, ZnO NPs possess various medicinal properties such as antimicrobial, antidiabetic[17], anti-inflammatory, anticancer[18], antioxidant, and wound healing properties[1]. United States Food and Drug Administration (US FDA) has considered ZnO as GRAS (generally recognized as safe) metal oxide[1]. Besides, zinc is an essential trace element in the human body, so it attracts a little attention during the assessment of NPs toxicity.

## MATERIALS AND METHOD

### Biosynthesis of ZnO NPs Using *Aloe vera* Leaves Extract

Fresh *Aloe vera* leaves were cut and washed by running tap water until all dust was removed and then washed by deionized water. Fifty grams of succulent leaves were supplemented to 100 ml of sterilized deionized water, blended for 5 min and remained in water bath at 60 ℃ for 20 min. The mixture was first filtered by cotton batch and then by filter paper for three times. The stock mixture of extract (50% w/v) was pale yellow colored.

Zinc nitrate [$Zn(NO_3)_2.6H_2O$] (Techno Pharmchem company, India) was prepared in concentration of 0.01 M. The plant extract was added to the zinc nitrate solution (1:4, respectively) with stirring at 40 ℃. Potassium hydroxide [KOH (1M)] was slowly added drop by drop to the mixture. The color of the mixture turned from clear bright yellow to a little turbid, and a white precipitate began to form. At this point, pH of the mixture was adjusted at 8 by using jenway pH meter (Cole-Parmer, Egypt). The mixture was cooled at room temperature and centrifuged by a centrifuge pro-K2015R (Wolflabs, UK) at 6000 rpm for 15 min at -4 ℃ to get the white precipitate. The precipitate was dried at 60 ℃ for 24 hrs and then calcinated at 400 ℃ for 4 hours to get a white powder of ZnO NPs.

### Characterization of Biosynthesized ZnO NPs

Characterization of ZnO NPs were performed as recommended by Mourdikoudis et al[20]. ZnO NPs were detected by V-770 UV-Vis/NIR Spectrophotometer (Jasco, UK) at wavelength range between 200 and 800 nm. X-ray Diffraction (XRD) analyzer (Bruker D8 Advance, Germany) provided information interpreting the nature of the phase, lattice parameters, crystalline structure and grain size of ZnO NPs. The crystalline grain size was estimated by the Scherrer equation[27] using the broadening of the most intense peaks of an XRD measurement. The structure was determined by comparing the position and intensity of the peaks to the reference patterns of joint committee on powder diffraction standards (JCPDS). Transmission Electron Microscopy (TEM) was used to analyze nanoparticle size and shape. Scanning Electron Microscopy (SEM) provided high resolution imaging of surfaces employed to characterize shapes and surface morphology. TEM and SEM images of ZnO NPs were taken in the electron microscopy unit at Assuit University. Fourier Transform Infrared (FTIR) of the

biosynthesized ZnO NPs was analyzed by FTIR spectroscopy (Bruker ALPHA Ⅱ, Germany) in the range of 4000–400 $cm^{-1}$ . The data was compared to a sample of *A. vera* extract, analyzed also by FTIR spectroscopy to identify the mutual functional groups between both of them which are responsible for the bio-reduction.

**Optimization of Biosynthesized ZnO NPs**

The optimization of ZnO NPs synthesis was performed considering 4 variables: zinc nitrate $Zn(NO_3)_2.6H_2O$ concentration, plant extract dilution, temperature, and pH value. The experiment included a negative control [a mixture of $Zn(NO_3)_2.6H_2O$ (0.01M) and KOH (1M)].

***Effect of Zinc Nitrate $Zn(NO_3)_2.6H2O$ Concentration***

Zinc nitrate was prepared in 11 different concentrations (0.001, 0.003, 0.005, 0.007, 0.009, 0.01, 0.03, 0.05, 0.07, 0.09, and 0.1 M). The stock *A. vera* leaves extract (50% w/v) was slowly added to each concentration of zinc nitrate solution with a percent of 1:4, respectively. All mixtures of extract and zinc nitrate solution were kept at room temperature 25±2 ℃. Potassium hydroxide [KOH (1 M)] was added to each mixture with stirring until the precipitate began to form.

***Effect of Plant Extract Dilution***

The stock *A. vera* leaves extract (50% w/v) was diluted to 4 different concentrations (40, 30, 20, and 10 %). Zinc nitrate was prepared in a concentration of 0.01 M. The extracts were separately added to the zinc nitrate solution in a percent of 1:4, respectively at room temperature 25 ± 2 ℃. Potassium hydroxide [KOH (1 M)] was added to each mixture with stirring until the precipitate began to form.

***Effect of Temperature***

Eight mixtures of stock *A. vera* leaves extract (50% w/v) and zinc nitrate solution (0.01M) were prepared in a percent of 1:4, respectively and incubated in eight water baths adjusted to different temperatures (room temperature 25±2, 40, 50, 60, 70, 80, 90, 100 ℃). Potassium hydroxide [KOH (1 M)] was added to each mixture with stirring until the precipitate began to form.

***Effect of pH Value***

Five mixtures of stock *A. vera* leaves extract (50% w/v) and zinc nitrate (0.01 M) were prepared by a percent of 1:4, respectively. The mixtures were separately adjusted to 5 different pH values (8, 9, 10, 11, and 12) by adding KOH (1 M) with stirring at room temperature 25 ± 2℃.

At the end, each mixture was centrifuged at 10000 rpm at -4 ℃ for 10 min to get the white precipitate to be monitored by UV-Vis spectroscopy between 200 and 800 nm.

**Testing The Antibacterial Impact of Biosynthesized ZnO NPs**

***Bacterial Isolates and Culture Conditions***

The bacterial isolates were isolated from urine samples of patients suspected to have urinary tract infections in three medical laboratories in Sohag governorate. The samples were streaked on cysteine lactose electrolyte-deficient agar, (C.L.E.D. agar w/bromo thymol blue M792-HiMedia Labs, India) and incubated at 35±2 ℃ for 18-24 hours. Examination of colony morphology, Gram staining, and biochemical tests were performed on each isolate according to the classification schemes described in Bergy᷈ s manual of determinative bacteriology[21]. The bacterial isolates were confirmed to be ESBL-producing Gram-negative and β-lactam-resistant Gram-positive isolates[22].

***Disk Diffusion Susceptibility Test***

The Kirby-Bauer disk diffusion susceptibility test[23] was performed based on the criteria described by clinical laboratory standards institute (CLSI)[24]. A 24-hrs growth of each bacterial isolate was adjusted to 0.5 McFarland standard and inoculated by streaking on Mueller Hinton agar (MHA–Accumix/Tulip Diagnostics Labs, India) plates. Different concentrations of ZnO NPs (1, 2, 3, 4, 5…etc.) mg/ml were prepared by dissolving the NPs in glycerol and water in percent 4:1, respectively and sonicated by sonicator Q700 (Terra universal, USA) for 10 minutes. 100 µl of each concentration were loaded on sterilized discs (5mm) and put on the MHA plates. Amoxicillin/clavulanate (20/10µg) discs

(Microxpress/Tulip Diagnostics Labs, India) were used as a positive control. Glycerol and water (4:1) discs were used as a negative control. The plates were incubated at 35±2 ℃ for 18-24 hrs. The diameters of zones of inhibition were measured in millimeters for each concentration, including the diameter of the disk.

***Broth Microdilution Assay***

The broth microdilution method was used to determine the lowest concentration of ZnO NPs that inhibits the visible growth of bacteria (minimum inhibitory concentration, MIC) and the lowest concentration that destroys all bacterial cells (minimum bactericidal concentration, MBC)[25]. The 96-well microtiter plate was performed based on the criteria described by CLSI[26]. Each well was inoculated with 50 µl of each concentration, 95 µl of nutrient broth medium, and 5 µl of bacterial suspension (0.5 McFarland standard). Well of growth control was inoculated with broth medium and bacterial suspension. Well of sterility control was inoculated with broth medium only. The plate was covered with a plate lid and incubated at 35±2 ℃ for 18-24 hrs. After the incubation period, the MIC was detected by Stat Fax-2100 microplate reader (Awareness Technology Inc, USA) as the lowest concentration of ZnO NPs that completely inhibited the growth of bacteria in the wells compared to the sterility control well. 100 µl of each well indicated no bacterial growth were transferred to MHA plate without ZnO NPs and incubated at 35±2 ℃ for another 18-24 hrs. The MBC was detected as the first concentration with no bacterial growth even in the absence of ZnO NPs effect.

## RESULTS AND DISCUSSION

### Results

### Biosynthesis of ZnO NPs Using *Aloe vera* Leaves Extract

Trying to explore the biosynthesis of NPs as a promising therapeutic alternative for antibiotics, ZnO NPs were the most considered for crucial reasons. Zinc is an essential trace element which is found in all tissues of human body. Zinc plays a pivotal functional role as a coenzyme. In addition, zinc plays a structural role whereas the zinc-finger structures provide a unique scaffold allowing the interaction of protein subdomains with DNA and other proteins. Although it is considered relatively nontoxic, free zinc ions can cause cytotoxic effects. Hence, ZnO NPs are synthesized to eliminate the cytotoxicity via bonding with a ligand. ZnO NPs are believed to be nontoxic, biosafe, and biocompatible[29].

In this study, the biosynthesis of ZnO NPs was remarkably simple and needed no additional costly equipment or precursors **(Fig. 1)**. Furthermore, it was observed that the plant-mediated process required short time and less energy where the reaction completed in less than one hour at moderate temperature. That was compatible with other studies supporting the green synthesis of NPs[11,12]. The plant-mediated synthesis was preferred as a simple method, cost effective, eco-friendly, and reduced in toxic byproducts[9]. In addition, phytochemicals which are responsible of the bio-reduction process of NPs function as both reducing and stabilizing agent; thus, there is no need to add any separate stabilizing agents[14]. In particular, *A. vera* plant was known for the presence of several active bio molecules such as tannins, saponins, phlobbasstannis, steroid, terpenoids, flavonoids, and glycosides[15,30]. These active biomolecules coat the NPs, providing them with specific medicinal properties through allowing several ligands-based conjugation with the receptors such as proteins, lipids, phospholipids, lipoteichoic acid present on the microbial membranes[31,32]. Besides, *A. vera* is highly prevalent and available all over the country.

The determinant of pH value (pH=8) and elevated temperature of calcination was critical for high solubility of ZnO NPs and enhancement of the antibacterial effect as recommended by Agarwal et al[32]. Because of the fact that the small NP are unstable compared to the larger one, calcination process was performed. Calcination involves heat treating of NPs so that they can fuse and enlarge their crystallite size[33]. The precipitate of ZnO NPs was calcinated at 400 ℃ according to Ismail et al. who confirmed that the ZnO NPs at 400 ℃ exhibited the best size with decreased agglomeration in addition to the best antimicrobial activity against both Gram-negative and Gram-positive bacteria compared to higher calcination temperatures[34].

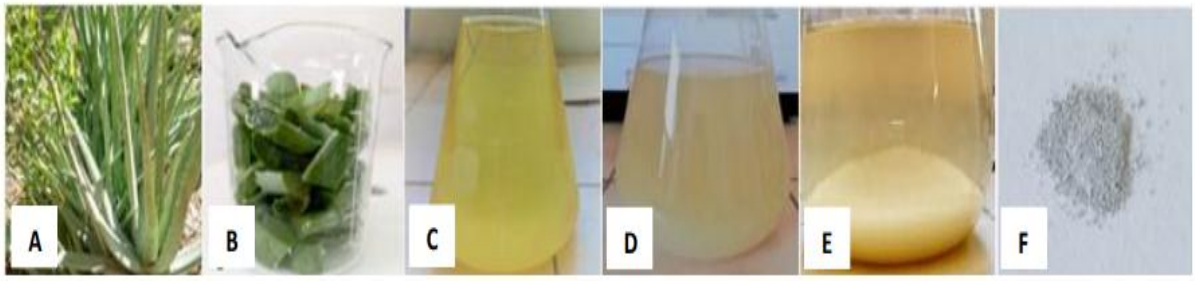


**Fig. 1:** Green synthesis of zinc oxide nanoparticles. (A) Fresh *Aloe vera* leaves were collected. (B) The leaves were washed and cut for preparing the extract. (C) The extract was added to the zinc nitrate solution. (D) KOH was slowly added to the mixture until the color of the mixture turned from clear bright yellow to a little turbid and a white precipitate began to form. (E) White ZnO NPs were totally precipitated. (F) White powder of ZnO NPs was obtained after calcination at 400◌̊ C.

**Characterization of Biosynthesized ZnO NPs**

The bio-reduction of $Zn^{2+}$ ion by *A. vera* leaves extract was detected using UV-Vis spectrophotometer at wavelength range of 200-800 nm and the intense peak of ZnO NPs was detected at wavelength of 383 nm with absorbance value of 5.71 (Fig. **2**). The formation of ZnO NPs was commonly detected at wavelengths range from 330 nm to 390 nm[35,36].

XRD analysis provided information about the crystalline structure of the biosynthesized ZnO NPs. The XRD planes of ZnO NPs [(100), (002), (101), (102), (110), (103), (200), (112), (201), (004) and (202)] showed highly intense, distinct and sharp peaks indicating the crystalline nature of ZnO NPs (Fig. **3**). The planes were indexed to a hexagonal wurtzite structure of ZnO with lattice parameters of $a_=$ 3.24 Å, $b_=$ 3.23 Å, $c_=$ 5.18 Å which matched with JCPDS card no. 36-1451[28]. XRD pattern confirmed that the ZnO NPs are highly crystalline with a hexagonal shape having a space group P63 mc (186) which characterized by two tetrahedrally bounded sublattices of $Zn^{2+}$ and $O^{2-}$ . The average crystallite size of ZnO NPs was calculated using Scherrer's equation: $D = 0.9\lambda/\beta \cos\theta$, where "λ" is the wavelength of X-ray, β is FWHM (full width at half maximum) in radians and θ diffraction angles. The average mean crystallite size was calculated to be 16.7 nm.

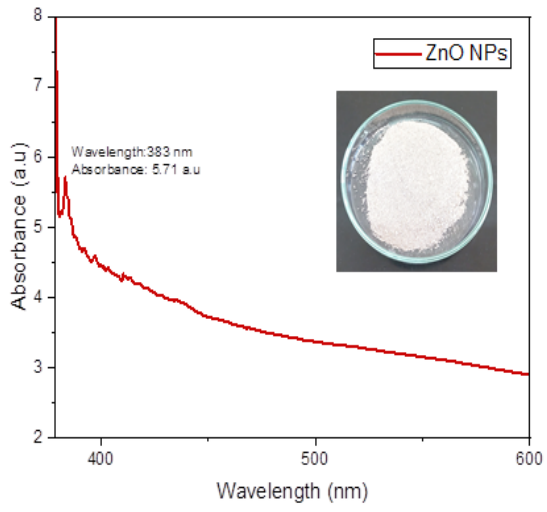


**Fig.2:** V–Vis spectrum of the biosynthesized ZnO-NPs.

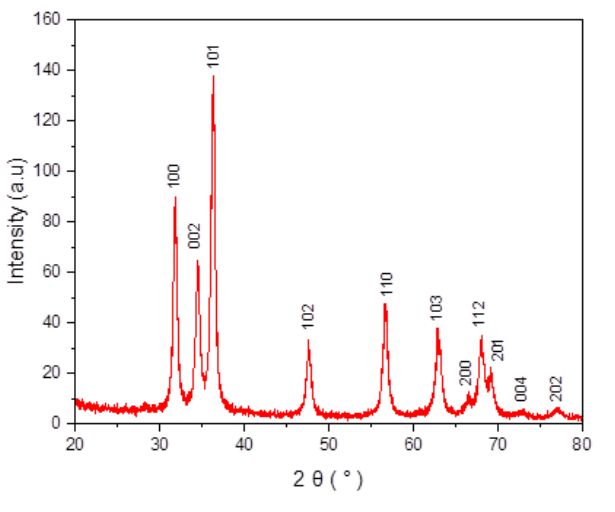


**Fig. 3:** XRD patterns of the biosynthesized ZnO NPs.

The morphology of the biosynthesized ZnO NPs was exhibited by transmission electron microscopy (Fig. **4**). The average mean particle size of ZnO NPs was ~ 20 nm. The morphology of the biosynthesized ZnO NPs was exhibited by scanning electron microscopy (Fig. **5**). The majority of ZnO NPs was hexagonal shaped. That was compatible with other studies that reported the hexagonal structure of ZnO NPs which were biosynthesized using *A. vera* leaves extract[23,43].

FTIR analysis was conducted separately on both *A. vera* leaves extract and the biosynthesized ZnO NPs to identify the mutual functional groups which might be responsible for the bio-reduction **(Fig. 6)**. The absorption bands of *A. vera* leaves extract and ZnO NPs in respect to the functional groups and possible phytocompounds are illustrated in **(Tables 1 and 2)**. The mutual presence of functional groups that characterize phenolic compounds (Glycosides/Flavonoids) suggested their principle role in the bio-reduction. Our results concurred with the observations of Ali et al.[37]. The prominent band position at 420 $cm^{-1}$ was distinctive of the vibrational bands of ZnO NPs as reported by Navas et al.[38]. Various active biomolecules detected on the surface of ZnO NPs can aid in their antibacterial activity through allowing multiple ligand-based conjugation with receptors on the bacterial membranes.

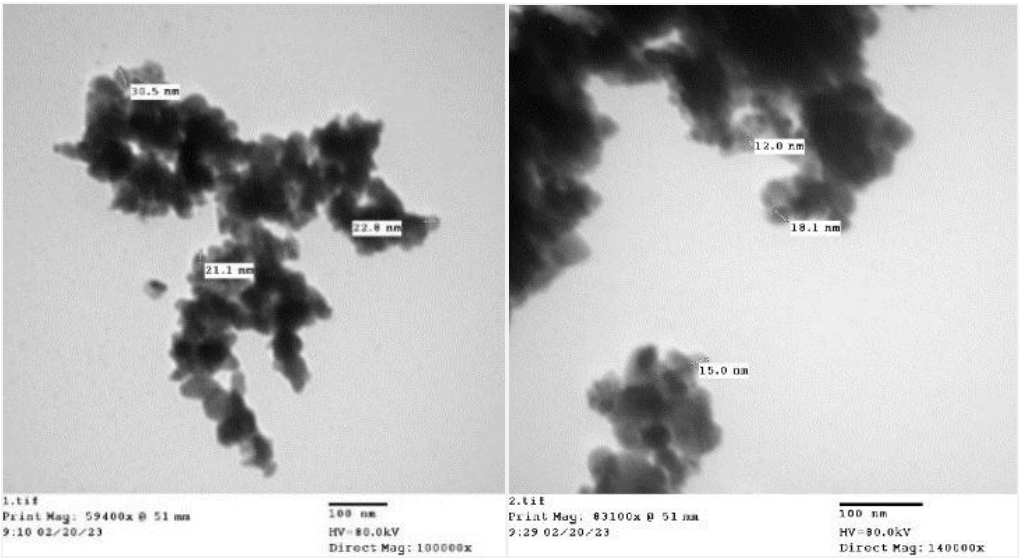


**Fig. 4:** The TEM images of the biosynthesized ZnO NPs.

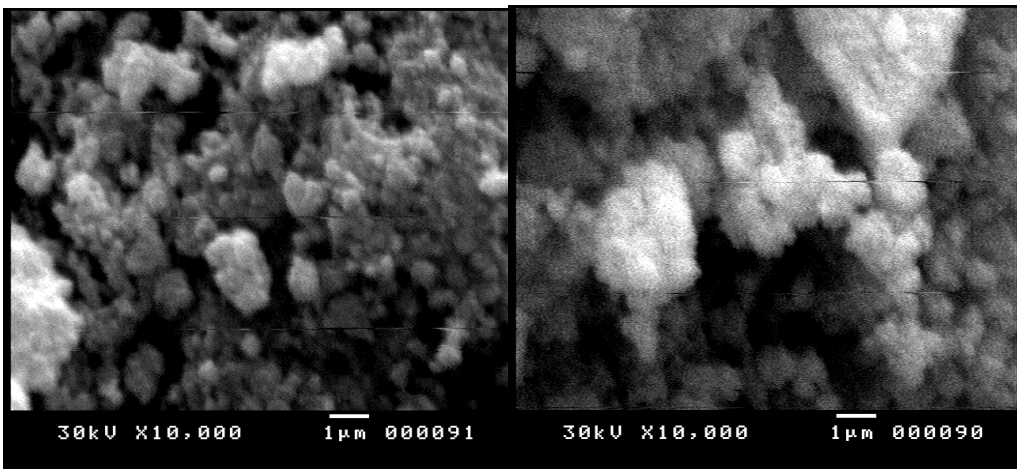


**Fig. 5:** The SEM images of the biosynthesized ZnO NPs.

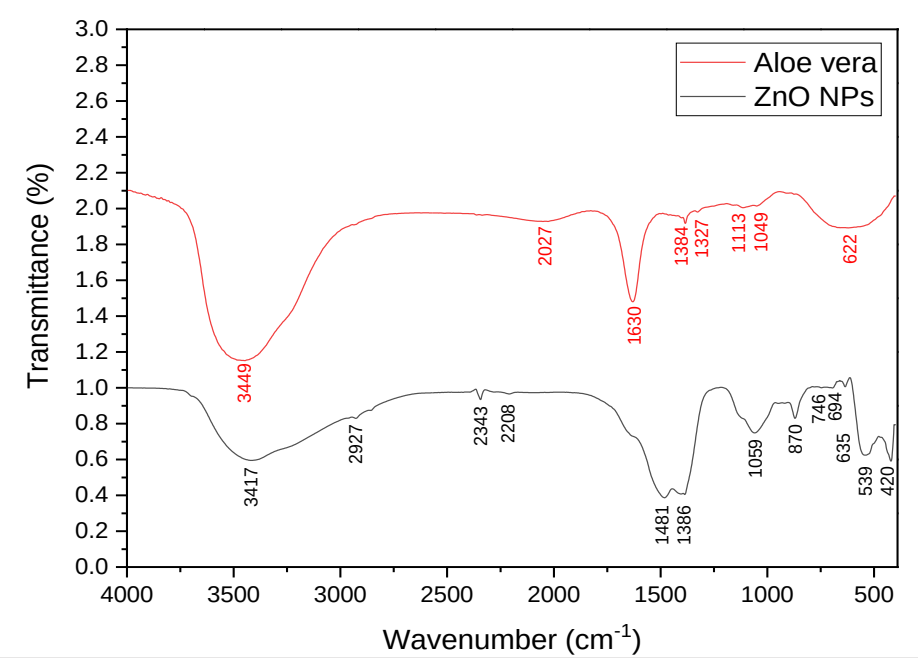


**Fig. 6:** FTIR spectra of *Aloe vera* leaves extract and the biosynthesized ZnO NPs

**Table 1**: Functional groups and possible phytocompounds of *Aloe vera* leaves extract.

| Wave Number ($Cm^{-1}$) | Functional Group/ Assignment | Possible Phytocompounds |
|---|---|---|
| 3449 | Phenolic OH-stretching | Glycosides/ Flavonoids |
| 2027 | N = C = S stretching | Isothiocyanate |
| 1630 | C = C stretching | Conjugated alkene |
| 1384 | S = O stretching | Sulfonyl chloride |
| 1327 | C - N stretching | Aromatic amine |
| 1113 | C - O stretching | Amino sugar glucosamine |
| 1049 | S = O stretching | sulfoxide compound |
| 622 | C - Cl stretching | Halo compound |

**Table 2**: Functional groups and possible phytocompounds of the biosynthesized ZnO NPs.

| Wave Number ($Cm^{-1}$) | Functional Group/ Assignment | Possible Phytocompounds |
|---|---|---|
| 3417 | Phenolic OH-stretching | Glycosides/ Flavonoids |
| 2927 | C - H stretching | Alkane |
| 2343 | O = C = O stretching | Carbon dioxide |
| 2208 | C ≡ C stretching | Alkyne |
| 1481 | C - H bending | Alkane |
| 1386 | S = O stretching | Sulfonyl chloride |
| 1059 | S = O stretching | Sulfoxide compound |
| 870 | C - H bending | Di/ tri substitution |
| 746 | C - H bending | Mono/ Di substitution |
| 694 | C = C stretching | Alkene |
| 635 | C - Cl stretching | Halo compound |
| 539 | C - Cl stretching | Halo compound |
| 420 | Zn - O stretching | ZnO NPs |

**Optimization of Biosynthesized ZnO NPs**

***Effect of Zinc Nitrate $Zn(NO_3)_2.6H2O$ Concentration***

The effect of 11 different concentrations of zinc nitrate Zn $(NO_3)_2.6H_2O$ was tested on the biosynthesis of ZnO NPs **(Fig. 7)**. UV-Vis spectra were monitored for the tested concentrations **(Fig. 8)** and showed that the higher yield production was at higher concentrations (0.09M and 0.1M) referring to two beaks at 375 nm and 374 nm, respectively. However, both concentrations showed broad beaks referring to larger size of ZnO NPs.

It was observed that the other concentrations less than 0.09 M showed convergent beaks and particularly, 0.01M and 0.03M showed approximately the same high yield so both of which were the most recommended concentrations for biosynthesis of ZnO NPs. Yusof et al. reported that the generation of ZnO NPs was significantly increased with higher zinc salt concentration, however it can lead to the agglomeration and formation of larger-sized ZnO NPs[39]. Moazzen et al. reported that the usage of lower concentration of zinc precursor can lead to the synthesis of smaller-sized ZnO NPs[40]. In addition, Alami et al. reported that the crystallite size of ZnO NPs increased in respect to zinc salt concentration (9.95, 27.40, and 32.35 nm for zinc precursor concentrations 0.05, 0.1, and 0.2 M, respectively) confirming that the size can be highly affected by the concentration of zinc salt[41].

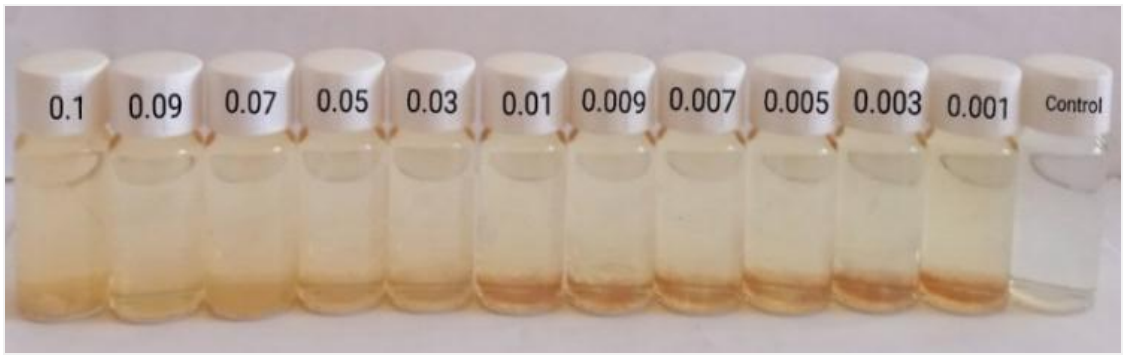


**Fig. 7:** Digital photograph showing the effect of 11 tested concentrations (0.001, 0.003, 0.005, 0.007, 0.009, 0.01, 0.03, 0.05, 0.07, 0.09, and 0.1 M) of zinc nitrate $Zn(NO_3)_2.6H_2O$ on the biosynthesis of ZnO NPs compared to a negative control.

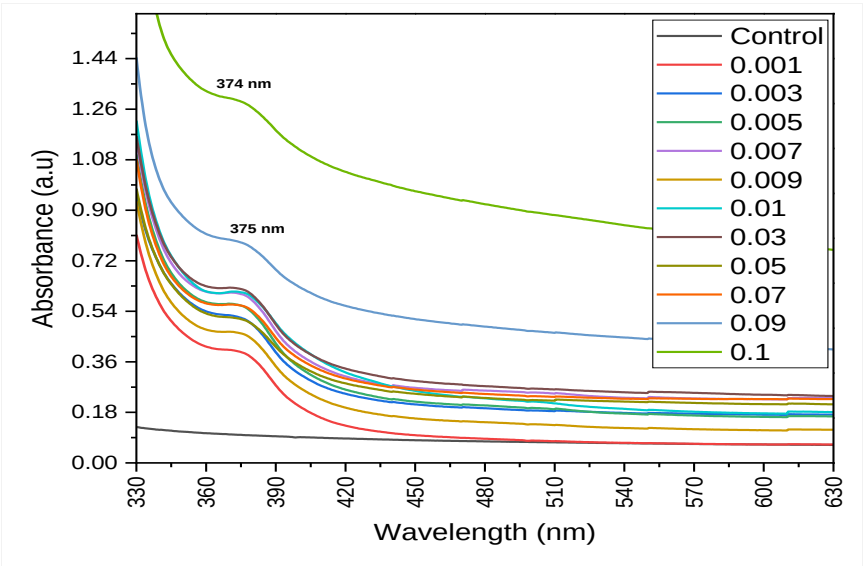


**Fig. 8:** UV-Vis spectra illustrating the effect of 11 tested concentrations of zinc nitrate $Zn(NO_3)_2.6H_2O$ on the biosynthesis of ZnO NPs compared to a negative control.

***Effect of Plant Extract Dilution***

The effect of 5 different dilutions of *A. vera* leaves extract was tested on the biosynthesis of ZnO NPs **(Fig. 9)**. It was observed by unaided eye that the precipitate was very tiny in plant extract dilutions beneath 50%. UV-Vis spectra were monitored for the tested dilutions of extracts **(Fig. 10)** and showed an increase in yield production of ZnO NPs in respect to the increase of extract concentration, particularly at 40% and 50% with significant beaks at 372 nm 9 and 371 nm, respectively. That was rational as the increase of plant extract concentration means an increase of the phytochemicals that are responsible for ZnO NPs formation. Jayachandran et al. reported that higher concentrations of plant extract led to high production of ZnO NPs[42]. Similarly, Sangeetha et al. observed that high production of ZnO NPs has been achieved using *Aloe barbadensis* concentration greater than 25%[43].

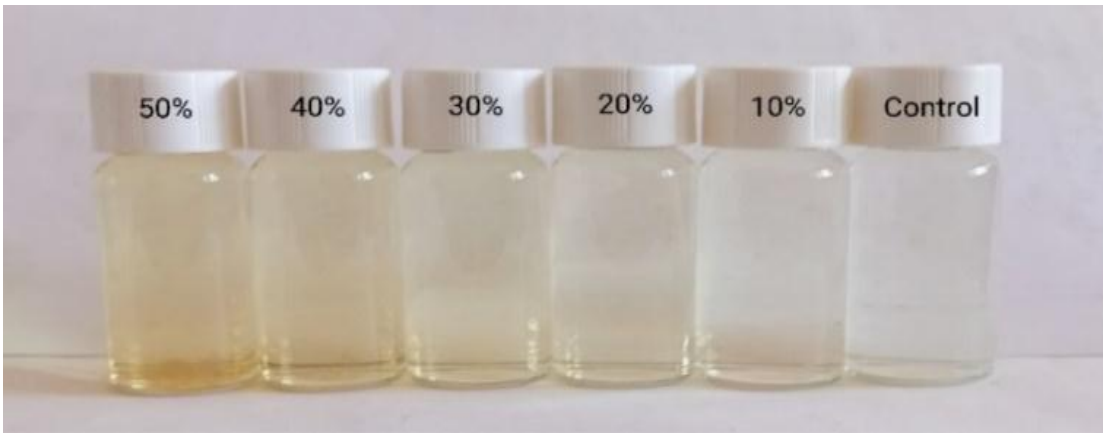


**Fig. 9:** Digital photograph showing the effect of 5 tested dilutions (50, 40, 30, 20, and 10 %) of *Aloe vera* plant extract on the biosynthesis of ZnO NPs compared to a negative control.

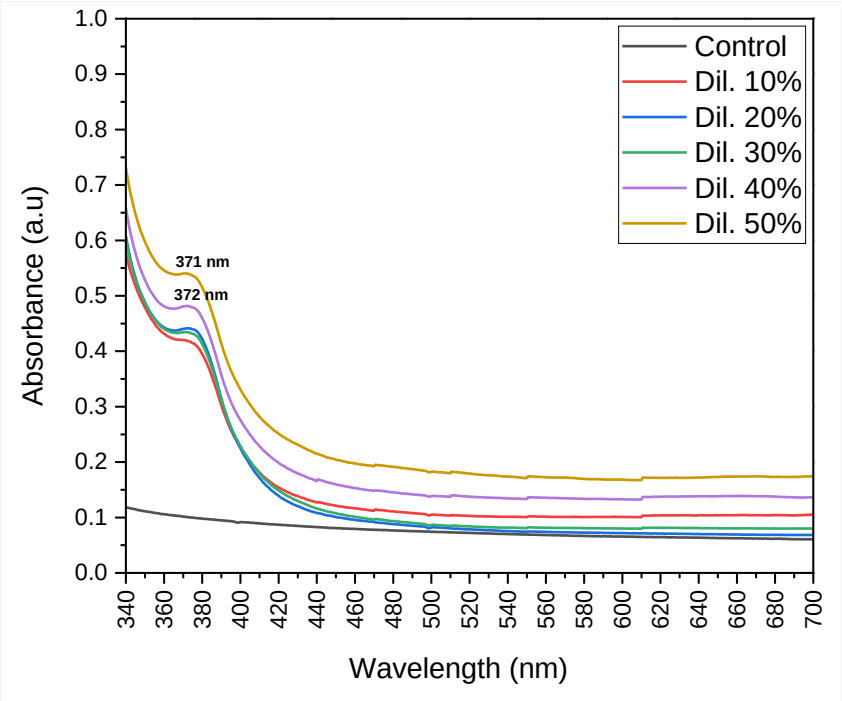


**Fig. 10:** UV-Vis spectra illustrating the effect of 5 tested dilutions of *Aloe vera* plant extract on the biosynthesis of ZnO NPs compared to a negative control**.**

***Effect of Temperature***

The effect of 8 degrees of temperature was tested on the biosynthesis of ZnO NPs **(Fig. 11).** UV-Vis spectra were monitored for the tested temperatures **(Fig. 12)**. Temperature plays a critical role in the biosynthesis of ZnO NPs affecting their size and quantity[4]. UV-Vis spectra showed 2 distinct beaks at T= 25±2 ℃ (373 nm) and 40 ℃ (372 nm) indicating smaller sizes of ZnO NPs compared to broad beaks of other temperatures. Higher temperatures showed larger yield and larger sizes of ZnO NPs. Equivalent results were obtained from Khan et al. who studied the synthesis of ZnO NPs at different temperatures. They observed the increase in the crystallite sizes of ZnO NPs in respect to increase of temperature and explained their observations according to the oriented attachment and Oswald ripening phenomena[44] both of which are induced in response to form more energetically-stable larger nanoparticles[33]. Similarly, other studies also reported the increase of the crystallite size of ZnO NPs in respect to the increase of temperatures[45,46].


**Fig. 11:** Digital photograph showing the effect of 8 tested temperatures (25±2, 40, 50, 60, 70, 80, 90, and 100 ℃) on the biosynthesis of ZnO NPs compared to a negative control.

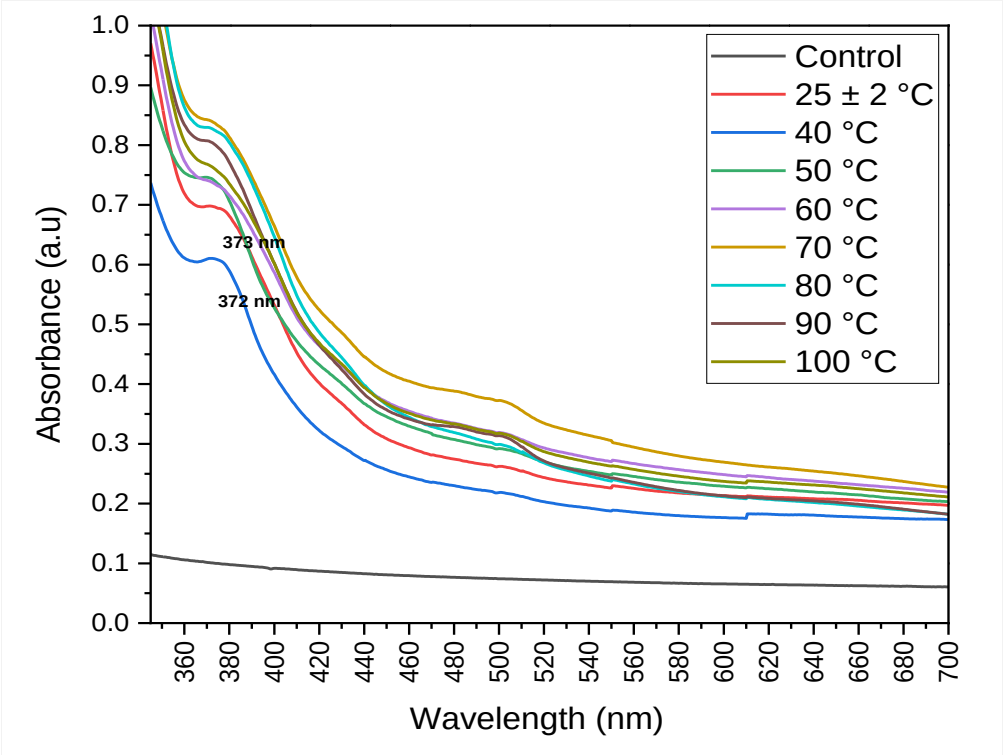


**Fig. 12:** UV-Vis spectra illustrating the effect of 8 tested temperatures on the biosynthesis of ZnO NPs compared to a negative control.

***Effect of pH Value***

The effect of 5 adjusted pH values was tested on the biosynthesis of ZnO NPs using KOH (1M) **(Fig. 13)**.

UV-Vis spectra were monitored for the adjusted pH values **(Fig. 14)**. pH value of the reaction could determine the crystallite size of ZnO NPs synthesized[33,39]. At pH = 8, the high percent of hydroxyl ions $OH^-$ causes strong attraction to positively-charged zinc ions $Zn^{2+}$ and subsequently, increase the crystallization and synthesis of smaller ZnO NPs.

Higher pH values accelerate the nucleation rate and result in higher yield, however, intermediate compounds (i.e., $Zn(OH)_2$ and $[Zn(OH)_4]^{2-}$) tend to form that lead to the synthesis of larger ZnO NPs. In the present study, UV-Vis spectra performed for the adjusted pH values showed distinct beak (364 nm) at pH=8 which indicated smaller size of ZnO NPs comparing to broad beaks of other pH values. In addition, the absorbance at pH=8 was 1.12 which reflected acceptable yield. Accordingly, the value of pH=8 was highly recommended based on our results. In agreement with our results, Saranya et al. observed that the optimum pH value of ZnO NPs synthesized via *Zea mays* extract was pH=8[47]. In addition, Jin et al. confirmed that the particle size of ZnO NPs was smaller with uniform dispersion at pH=8.5[48]. Arya et al. reported that the crystallite size of ZnO NPs was 17.44 nm at pH=8 with moderate yield compared to 74.04 nm ZnO NPs synthesized at pH=12[49].

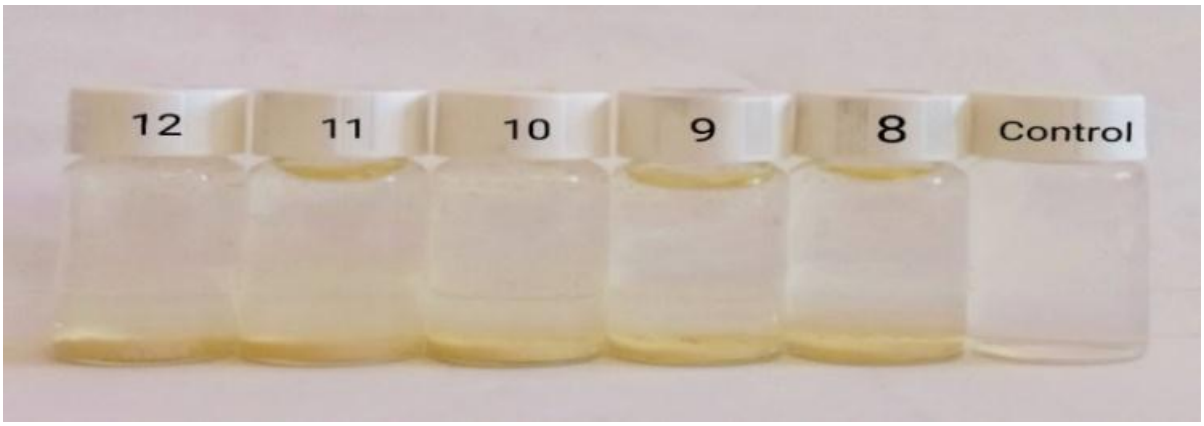


**Fig. 13:** Digital photograph showing the effect of 5 tested pH values (8, 9, 10, 11, and 12) on the biosynthesis of ZnO NPs compared to a negative control.

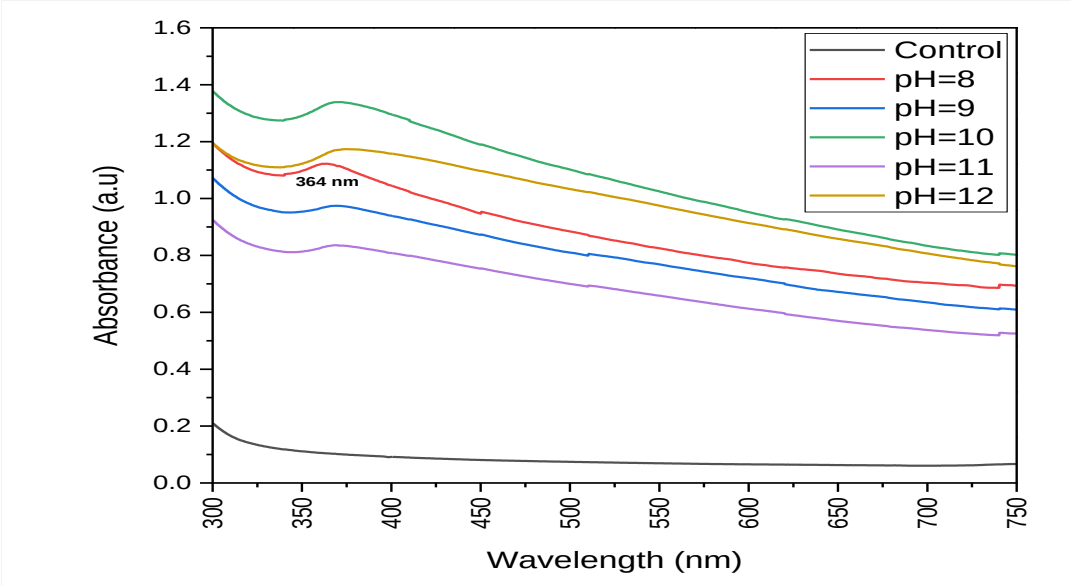


**Fig. 14:** UV-Vis spectra illustrating the effect of 5 tested pH values on the biosynthesis of ZnO NPs compared to a negative control.

**Testing The Antibacterial Impact of Biosynthesized ZnO NPs**

***Bacterial Isolates and Culture Conditions***

ESBL-producing Gram-negative isolates were confirmed to be *Escherichia coli*, *Klebsiella pneumonia*, *Citrobacter koseri*, *Serratia fonticola*, *Proteus mirabilis*, and *Pseudomonas aeruginosa*[22]. β-lactam-resistant Gram-positive isolates were *Enterococcus faecalis*, *Streptococcus mitis*, *Corynebacterium urealyticum*, and *Bacillus cereus*[22].

***Disk Diffusion Susceptibility Test***

Glycerol was particularly selected to dissolve ZnO NPs due to its low toxicity. Besides, it was observed through experiments that glycerol increased the dispersion of ZnO NPs more than dimethyl sulfoxide (DMSO). Cristino et al. recommended the use of glycerol as a solvent and a co-solvent with any other polar solvent such as water for the dispersion of metal oxide nanoparticles that presented catalytic abilities and increased their lifetime[50].

The concentrations of ZnO NPs were tested on ESBL-producing Gram-negative and β-lactam resistant Gram-positive bacteria compared to amoxicillin/clavulanate (20/10 μg) disc as a positive control and glycerol and water (4:1) disc as a negative control **(Fig. 15).** The diameters of zones of inhibition for each concentration were measured **(Tables 3 and 4)** showing the response of all bacterial isolates to ZnO NPs. Our results were compatible with other studies that reported the antibacterial activity of ZnO NPs[37,51,52]. In particular, Gad El-Rab et al. reported that ZnO NPs managed to inhibit ESBL-producing uropathogens including *E. coli* and *K. pneumonia*[69].

An important factor which can affect the antibacterial activity of ZnO NPs is their concentration[53]. Concentration of ZnO NPs is proportional to their antibacterial effect[32]. In our study, it was observed that the inhibition zones increased in respect to the increase of ZnO NPs concentration. In agreement with our results, Karvani and Chehrazi reported that increasing of ZnO NPs concentration from 0.0195 to 10 mg/ml increased the inhibition zones in case of *E. coli* and *S. aureus* to 28mm and 22mm, respectively[54].

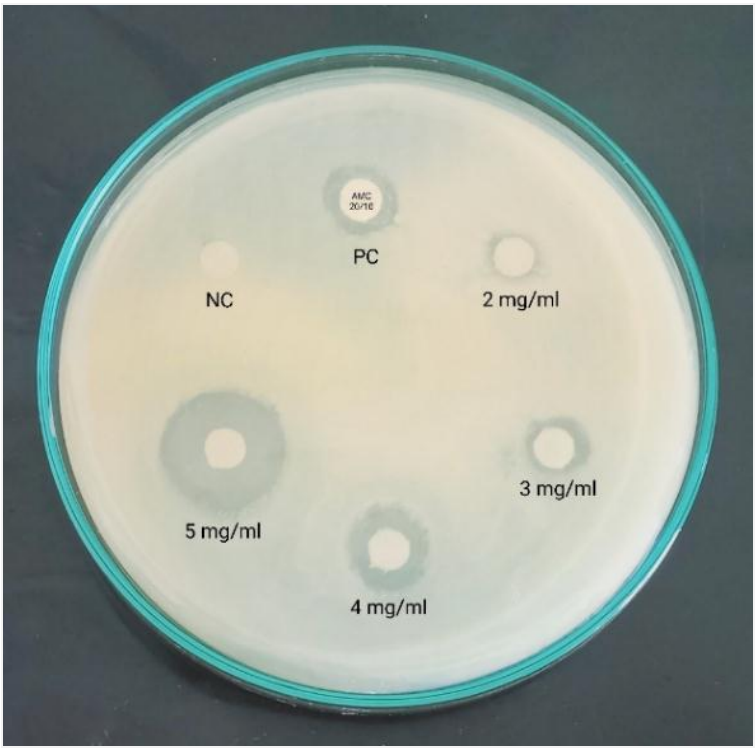


**Fig. 15:** Antibacterial impact of different concentrations of ZnO NPs on *E. coli* isolate compared to amoxicillin/clavulanate (20/10 μg) disc as a positive control "PC" and glycerol and water (4:1) as a negative control "NC".

**Table 3:** Antibacterial effect of ZnO NPs against gram-negative isolates.

| Bacterial Isolate | Zone of Inhibition (mm) Per Concentration | | | | | MIC (mg/ml) | MBC (mg/ml) |
|---|---|---|---|---|---|---|---|
| | **1 mg/ml** | **2 mg/ml** | **3 mg/ml** | **4 mg/ml** | **5 mg/ml** | | |
| ***E. coli*** | NZ | 6 ± 1 | 9.67 ± 0.58 | 14.67 ± 1.53 | 23.33 ± 1.15 | 2 | 4 |
| ***K. pneumonia*** | NZ | NZ | 13.67 ± 0.58 | 18.67 ± 0.58 | 30 ± 1 | 2.2 | 3.2 |
| ***C. koseri*** | NZ | 6.67 ± 0.58 | 12 ± 1 | 16.33 ± 0.58 | 25 ± 1 | 2 | 3.6 |
| ***S. fonticola*** | NZ | NZ | 16 ± 1 | 18.33 ± 0.58 | 22.67 ± 1.53 | 2.1 | 2.1 |
| ***P. mirabilis*** | NZ | NZ | NZ | NZ | 20.67 ± 1.15 | 4.1 | 4.7 |
| ***P.aeruginosa*** | NZ | NZ | NZ | NZ | 20 ± 1 | 4.1 | 4.3 |

NZ = no zone of inhibition.

**Table 4**: -Antibacterial effect of ZnO NPs against gram-positive isolates.

| Bacterial Isolate | Zone of Inhibition (mm) Per Concentration | | | | | MIC (mg/ml) | MBC (mg/ml) |
|---|---|---|---|---|---|---|---|
| | **8 mg/ml** | **9 mg/ml** | **10 mg/ml** | **11 mg/ml** | **12 mg/ml** | | |
| ***E. faecalis*** | NZ | NZ | 8.33 ± 0.57 | 16.67 ± 0.58 | 23.67 ± 0.57 | 10 | 10.8 |
| ***S. mitis*** | NZ | 15.67 ± 0.58 | 23.33 ± 1.15 | 28.67 ± 0.58 | 36.67 ± 1.15 | 8.2 | 8.2 |
| ***C.urealyticum*** | NZ | NZ | NZ | 8.33 ± 0.58 | 19.67 ± 0.58 | 11 | 11.4 |
| ***B. cereus*** | NZ | NZ | NZ | 15.67 ± 1.53 | 26 ± 1 | 10.6 | 11 |

NZ = no zone of inhibition.

***Broth Microdilution Assay***

ZnO NPs represented promising therapeutic molecules with broad spectrum antibacterial activity including exhibition of bactericidal effect on Gram-negative bacteria (*E. coli*, *K. pneumonia*, *C. koseri*, *S. fonticola*, *P. mirabilis*, and *P. aeruginosa*) and Gram-positive bacteria (*E. faecalis*, *S. mitis*, *C. urealyticum*, and *B. cereus*). Values of MIC and MBC of ZnO NPs against Gram-negative and Gram-positive bacteria were listed in **(Tables 3, 4)**. Values of MIC and MBC of ZnO NPs varied to be 2-4.1 mg/ml and 2.1-4.7 mg/ml, respectively for Gram-negative bacterial isolates. Furthermore, values of MIC and MBC of ZnO NPs varied to be 8.2-11 mg/ml and 8.2-11.4 mg/ml, respectively for Gram-positive bacterial isolates. Similarly, Lakshmi et al. observed that the MIC values for ZnO NPs synthesized using *A. vera* extract ranged among 3-5 mg/ml against Gram-negative bacteria[55] Khatana et al. reported various Gram-negative and Gram-positive isolates that were susceptible to ZnO NPs synthesized using *Aloe vera* extract[56]. In addition, other studies confirmed the antibacterial activity of ZnO NPs on various bacterial isolates[57-59].

The NPs could be competitors to antibiotics as they act on different pathways that antibiotics are unable to target. Significantly, the principle mechanisms of antibiotic resistance are irrelevant to NPs as they do not necessarily involve their internalization. In particular, the antibacterial impact of ZnO NPs could be adopted through distinct mechanisms. The oxidative stress induced by reactive oxygen species ROS ($O^{2-\bullet}$, $OH^{-\bullet}$, and $H_2O_2$.) is a critical mechanism that is responsible for the antimicrobial effect of NPs by integrating the destruction of cellular components such as DNA, lipids, and proteins. Another antimicrobial mechanism is the release of zinc ions $Zn^{2+}$ while ZnO NPs are in dissolution. Zinc ions contribute to decrease amino acid metabolism and disturb the enzymatic system[32].

Another important antibacterial mechanism of ZnO NPs refers to the interaction of ZnO NPs with the bacterial cell wall, leading to the loss of the bacterial integrity. The cell wall of Gram-positive bacteria consists of a rigid thick layer of peptidoglycan (20-80 nm) which provides a protective barrier for the cell compared to the thin peptidoglycan layer (5-10 nm) of Gram-negative bacteria that may facilitate the entrance NPs and the rupture of bacterial cell[60]. Brayner et al. evaluated the antibacterial effect of ZnO NPs on *E. coli* and indicated the damaged bacterial cells due to disorganization of the membrane as well as NPs internalization[61]. SEM images reported by Zhang et al. confirmed the damage of *E. Coli* membrane upon direct interaction with ZnO NPs[62]. Other studies reported that the differences in susceptibility to ZnO NPs with maximum inhibition zone against *E. coli* more than *S. aureus* refer to the differences in their cell wall[59,63,64]. That could explain the higher susceptibility of Gram-negative isolates (MIC= 2-4.1 mg/ml) to ZnO NPs than Gram-positive isolates (MIC= 8.2-11 mg/ml) in our study.

The antibacterial activity of ZnO NPs can be altered considering their size. The antibacterial effect of smaller-sized NPs is hypothesized to cause an increase in cell death. Raghupathi et al. studied the antibacterial activity of ZnO NPs and observed that the viability of the bacterial cell significantly decreased upon particle size decreasing from 212 to 12 nm[57]. Since ROS generation and zinc ions release depend strongly on surface area, smaller ZnO NPs with a larger surface area to volume ratio can penetrate the bacterial membrane more easily due to increased surface reactivity. In addition, the need for more small-sized NPs to cover the bacterial colony leads to the generation of high concentrations of ROS released which subsequently damage and inactivate cellular biomolecules.

Furthermore, smaller-sized NPs can participate in the subcellular reactions as their size is comparable to the macromolecules such as large protein complexes[60]. Through our results, it was observed that the biosynthesized ZnO NPs had relatively small size with a median crystallite size of 16.7 nm and a median particle size of ~ 20 nm. Subsequently, it was believed that the small size of ZnO NPs contributed to the bactericidal impact on a wide range of uropathogenic bacterial isolates tested in our study.

Another parameter which can affect the antibacterial impact of ZnO NPs is their morphology. In our study, TEM and SEM images showed that he majority of ZnO NPs was hexagonal shaped. The shape-dependent effect is explained in terms of nanoparticle active facets. The higher number of active facets of ZnO NPs possess higher amount of oxygen vacancies that cause an increase of ROS generation and an enhancement of NPs internalization. Due to its unsaturated oxygen coordination and positive charge, the (001) face in the hexagonal faceted structure of ZnO NP can adsorb oxygen molecules and $OH^-$ ions that results in a high generation of ROS, and hence increases the antimicrobial effect[65,66]. In addition, the presence of corners and edges in ZnO NPs can lead to an increase in the toxicity due to the increased reactive surface sites that help in the adsorption and binding of compounds. Padmavathy and Vijayaraghavan suggested that the antibacterial effect of ZnO NPs referred to the edges and corners of their surface causing the membrane injury[67].

Another significant parameter is the presence of halogen included in the ZnO NPs structure. Two absorption bands were detected in FTIR analysis of ZnO NPs at 635 $cm^{-1}$ and 539 $cm^{-1}$ (Table **2**) that indicated nothing but halo compounds. Similarly, a study reported that MgO NPs synthesized (using an aerogel of $Cl_2$ and $Br_2$) were active against Gram-negative and Gram-positive bacteria due to the oxidizing power of halogen[68].

## Conclusion

Development of nanotechnology guarantees a new chance to combat drug-resistant bacteria and related infections and diseases. In this study, ZnO NPs were synthesized via a simple green approach. The biosynthesis-related conditions including zinc nitrate concentration of 0.01M, *Aloe vera* leaves extract concentration of 50%, pH=8, and 40 ℃ were adjusted to get ZnO NPs with smaller sizes. Significantly, the biosynthesized ZnO NPs exhibited a broad spectrum bactericidal impact against both Gram-negative and Gram-positive bacteria. Future perspective of the green-synthesized ZnO NPs should

consider further investigations for the extension from *in vitro* experiments to the real treatment.

## REFERENCES


1. H. Agarwal, S. Kumar and S. Rajeshkumar, "A Review on Green Synthesis of Zinc Oxide Nanoparticles: An Eco-friendly Approach", ***Res Efficient Tech***, 3(4), 406-413(2017).
2. M. Akhtar, M. Swamy, A. Umar and A. Al Sahli, "Biosynthesis and Characterization of Silver Nanoparticles from Methanol Leaf Extract of *Cassia didymobotyra* and Assessment of Their Antioxidant and Antibacterial Activities", ***J Nanosci Nanotech***, 15(12), 9818-9823(2015).
3. G. Rudramurthy, M. Swamy, U. Sinniah and A. Ghasemzadeh, "Nanoparticles: Alternatives Against Drug-Resistant Pathogenic Microbes", ***Molecules***, 21(7), 836-866(2016).
4. F. Thakral, G. Bhatia, H. Tuli, A. Sharma and S. Sood, "Zinc Oxide Nanoparticles: from Biosynthesis, Characterization, and Optimization to Synergistic Antibacterial Potential, " ***Curr Pharm Rep***, 7, 15-25(2021).
5. J. Singh, T. Dutta, K. Kim, M. Rawat, P. Samddar and P. Kumar, "Green Synthesis of Metals and Their Oxide Nanoparticles: Applications For Environmental Remediation", ***J Nanobiotechnology***, 16(1), 16-84(2018).
6. D. Gupta, A. Boora, A. Thakur and T. Gupta, "Green and Sustainable Synthesis of Nanomaterials: Recent Advancements and Limitations", ***Env Res***, 231(3), 116316(2023).
7. N. Pavithra, K. Lingaraju, G. Raghu and G. Nagaraju, "*Citrus Maxima* (Pomelo) Juice Mediated Eco-Friendly Synthesis of ZnO Nanoparticles: Applications to Photocatalytic, Electrochemical Sensor and Antibacterial Activities", ***Spectrochim Acta A Mol Biomol Spectrosc***, 185, 11-19(2017).
8. R. Joerger, T. Klaus and C. Granqvist, "Biologically Produced Silver-Carbon Composite Materials for Optically Functional Thin-Film Coatings", ***Adv Mat***, 12(6), 407-409(2000).
9. J. Patra and K. Baek, "Green Nanobiotechnology: Factors Affecting Synthesis and Characterization Techniques", ***J Nanomat***, 2014(6), 1-12(2014).
10. K. Thakkar, S. Mhatre and R. Parikh, "Biological Synthesis of Metallic Nanoparticles", ***Nanomed Nanotech Biol Med***, 6(2), 257-262 (2010).
11. S. Iravani, "Green Synthesis of Metal Nanoparticles Using Plants", ***Green Chem***, 13(10), 2638-2650(2011).
12. K. Elumalai and S. Velmurugan, "Green Synthesis, Characterization and Antimicrobial Activities of Zinc Oxide Nanoparticles from The Leaf Extract of *Azadirachta Indica* (L.)", ***Appl Surf Sci***, 345, 329-336 (2015).
13. N. Asmathunisha and K. Kathiresan, "A Review on Biosynthesis of Nanoparticles by Marine Organisms", ***Coll Surf B: Biointerfaces***, 103(12), 283-287(2013).
14. K. Vijayaraghavan and T. Ashokkumar, "Plant-Mediated Biosynthesis of Metallic Nanoparticles: A Review of Literature, Factors Affecting Synthesis, Characterization Techniques and Applications", ***J Envir Chem Eng***, 5(5), 4866-4883(2017).
15. B. Raad, S. Ali, K. Rehman, N. Akhtar, B. Ullah and S. Wali, "Phytochemical Screening and Biological Activities of *Aloe vera* (L.) Burm", ***Pure Appl Biol***, 10, 360-367(2021).
16. M. Osmond and M. McCall, "Zinc Oxide Nanoparticles In Modern Sunscreens: An Analysis of Potential Exposure and Hazard", ***Nanotoxicology***, 4(1), 15-41(2010).
17. S. Gunalan, R. Sivaraja and V. Rajendran, "Green Synthesized ZnO Nanoparticles Against Bacterial and Fungal Pathogens", ***Prog Nat Sci: Mat Inter***, 22(6), 693-700(2012).
18. D. Suresh, Udayabhanu, P. Nethravathi, K. Lingaraju, H. Rajanaika, S. Sharma and H. Nagabhushana, "EGCG Assisted Green Synthesis of ZnO Nanopowders: Photodegradative, Antimicrobial and

Antioxidant Activities", ***Spectrochim Acta***, 136(1), 1467-1474(2015).

19. Y. Huang, C. Wu and R. Aronstam, "Toxicity of Transition Metal Oxide Nanoparticles: Recent Insights from In-vitro Studies", ***Materials***, 3(10), 4842-4859(2010).
20. S. Mourdikoudis, R. Pallares and N. Thanh, "Characterization Techniques for Nanoparticles: Comparison and Complementarity Upon Studying Nanoparticle Properties", ***Nanoscale***, 10(27), 12871-12934(2018).
21. R. Breed, E. Murray and N. Smith, "Bergey's Manual of Determinative Bacteriology", ***Baltimore, Williams & Wilkins Co***, 7th Edition (1957).
22. M. Abu-Gharbia, G. Al-Arabi and J. Salem, "Community-Acquired Urinary Tract Infections: Epidemiology, Etiology, and β-lactam Resistance", ***S J Sci***, 9(1), 47-55(2024).
23. A. Bauer, D. Perry and W. Kirby, "Single-Disk Antibiotic-Sensitivity Testing of *Staphylococci*: An Analysis of Technique and Results", ***AMA Arch Inter Med***, 104(2), 208-216(1959).
24. "M100: Performance Standards for Antimicrobial Susceptibility Testing", ***CLSI***, 30th Edition. 40 (2020).
25. I. Wiegand, K. Hilpert and R. Hancock, "Agar and Broth Dilution Methods to Determine the Minimal Inhibitory Concentration (MIC) of Antimicrobial Substances", ***Nat Protoc***, 3(2), 163-175(2008).
26. "M07-A10: Methods for Dilution Antimicrobial Susceptibility Tests for Bacteria That Grow Aerobically; Approved Standard", ***CLSI***, 10th Edition. 35 (2015).
27. P. Scherrer, "Determination of The Size and Internal Structure of Colloid Particles Using X-ray. News from the Society of Sciences in Göttingen", ***J Math Phys***, 98-100 (1918).
28. J. Chauhan, "Nanomaterial Doping, Synthesis and Characterization of Mn/Fe/Co/Ni/Cu Doped ZnO", ***Evincepub Pub***, (2020).
29. S. Gudkov, D. Burmistrov, D. Serov, M. Rebezov, A. Semenova and A. Lisitsyn, "A Mini Review of Antibacterial Properties of ZnO Nanoparticles", ***Front Phys***, 9, 641481(2021).
30. A. El Shafey, "Green Synthesis of Metal and Metal Oxide Nanoparticles From Plant Leaf Extracts and Their Applications: A Review", ***Green Process Synth***, 9(1), 304-339(2020).
31. K. Gudikandula and S. Maringanti, "Synthesis of Silver Nanoparticles by Chemical and Biological Methods and Their Antimicrobial Properties", ***J Exp Nanosci***, 11(9), 714-721(2016).
32. H. Agarwal, S. Menon, S. Kumar and S. Rajeshkumar, "Mechanistic Study on Antibacterial Action of Zinc Oxide Nanoparticles Synthesized Using Green Route", ***Chem Biol Interact***, 286(4), 60-70(2018).
33. E. Shaba, J. Jacob, J. Tijani and M. Suleiman, "A Critical Review of Synthesis Parameters Affecting The Properties of Zinc Oxide Nanoparticle and Its Application in Wastewater Treatment", ***Appl Water Sci***, 11(2), 48(2021).
34. A. Ismail, A. Menazea, H. Kabary, A. El-Sherbiny and A. Samy, "The Influence of Calcination Temperature on Structural and Antimicrobial Characteristics of Zinc Oxide Nanoparticles Synthesized by Sol-Gel Method", ***J Mol Struct***, 1196, 332-337(2019).
35. H. Mofid, M. Sadjadi, M. Sadr, A. Banaei and N. Farhadyar, "Synthesis of Zinc Oxide Nanoparticles Using *Aloe Vera* Plant For Investigation of Antibacterial Properties", ***Adv Nanochem***, 1, 32-35(2020).
36. M. Batool, S. Khurshid, Z. Qureshi and W. Daoush, "Adsorption, Antimicrobial and Wound Healing Activities of Biosynthesized Zinc Oxide Nanoparticles", ***Chem Pap***, 75, 893-907 (2021).
37. K. Ali, S. Dwivedi, A. Azam, Q. Saquib, M. Al-Said, A. Alkhedhairy and J. Musarrat, "*Aloe vera* Extract Functionalized Zinc Oxide Nanoparticles As Nano antibiotics Against Multi-Drug Resistant Clinical Bacterial Isolates", ***J Coll Inter Sci***, 472, 145-156 (2016).

38. D. Navas, A. Ibanez, I. Gonzalez, J. Palma and P. Dreyse, "Controlled Dispersion of ZnO Nanoparticles Produced By Basic Precipitation in Solvothermal Processes", ***Heliyon***, 6, e05821 (2020).
39. H. Yusof, N. Abdul-Rahman, R. Mohamad, U. Zaidan and A. Samsudin, "Optimization of Biosynthesis Zinc Oxide Nanoparticles: Desirability-Function Based Response Surface Methodology, Physicochemical Characteristics, and Its Antioxidant Properties", ***Open Nano***, 8, 100-106 (2022).
40. M. Moazzen, S. Borghei and F. Talesh, "Change in The Morphology of ZnO Nanoparticles Upon Changing The Reactant Concentration", ***Appl Nanosci***, 3, 295-302 (2013).
41. Z. Alami, M. Salem, M. Gaidi and J. Elkhamkhami, "Effect of Zn Concentration on Structural and Optical Proprieties of ZnO Thin Films Deposited By Spray Pyrolysis", ***Adv Ener Inter J***, 2(4), 11-24 (2015).
42. A. Jayachandran, T. Aswathy and A. Nair, "Green Synthesis and Characterization of Zinc Oxide Nanoparticles Using *Cayratia Pedata* Leaf Extract", ***Biochem Biophy Rep***, 26, 100995 (2021).
43. G. Sangeetha, S. Rajeshwari and R. Venckatesh, "Green Synthesis of Zinc Oxide Nanoparticles by *Aloe barbadensis* Leaf Extract: Structure and Optical Properties", ***Mater Res Bull***, 46(12), 2560-2566 (2011).
44. M. Khan, M. Hameedullah, A. Ansari, E. Ahmad, M. Lohani, R. Khan, M. Alam, W. Khan, F. Husain and I. Ahmad, "Flower-Shaped ZnO Nanoparticles Synthesized by A Novel Approach At Near-Room Temperatures With Antibacterial and Antifungal Properties", ***Inter J Nanomed***, 9, 853-864 (2014).
45. U. Manzoor, F. Zahra, S. Rafique, M. Moin and M. Mujahid, "Effect of Synthesis Temperature, Nucleation Time, and Postsynthesis Heat Treatment of ZnO Nanoparticles and Its Sensing Properties", ***J Nanomater***, 2015, Article ID 189058 (2015).
46. C. Pelicanoa, E. Magdaluyob and A. Ishizumi, "Temperature Dependence of Structural and Optical Properties of ZnO Nanoparticles Formed by Simple Precipitation Method", ***MATEC Web Conf***, 43, 02001 (2016).
47. S. Saranya, A. Eswari, E. Gayathri, S. Eswari and K. Vijayarani, "Green Synthesis of Metallic Nanoparticles using Aqueous Plant Extract and their Antibacterial Activity", ***Inter J Cur Mic Appl Sci***, 6, 1834-1845 (2017).
48. J. Jin, A. Hao, G. Wang, X. He, W. Zhang and Q. Chen, "The Study of Different pH Values on Morphology of ZnO Nanoparticles Via Sol-Gel Technology", ***J Chem Pharm Res***, 6(6), 1676-1680 (2014).
49. S. Arya, P. Mahajan, S. Mahajan, A. Khosla, R. Datt, V. Gupta, S. Young and S. Oruganti, "Review—Influence of Processing Parameters to Control Morphology and Optical Properties of Sol-Gel Synthesized ZnO Nanoparticles", ***ECS J Solid State Sci Tech***, 10, 023002 (2021).
50. A. Cristino, I. Matias, D. Bastos, R. Santos, A. Ribeiro and L. Martins, "Glycerol Role in Nano Oxides Synthesis and Catalysis", ***Catalysts***, 10 (2020).
51. S. Mustafa, H. Khan, I. Shukla, F. Shujatullah, M. Shahid, M. Ashfaq and A. Azam, "Effect of ZnO Nanoparticles on ESBL Producing *Escherichia coli* & *Klebsiella spp.*", ***East J Med***, 16(2011), 253-257 (2011).
52. M. Maruthupandy, G. Rajivgandhi, T. Muneeswaran and J. Song, "Biologically Synthesized Zinc Oxide Nanoparticles As Nano antibiotics Against ESBLs Producing Gram Negative Bacteria", ***Microb Pathog***, 121, 224-231 (2018).
53. A. Król, P. Pomastowski, K. Rafińska, V. Plugaru and B. Buszewski, "Zinc Oxide Nanoparticles: Synthesis, Antiseptic Activity and Toxicity Mechanism", ***Adv Colloid Inter Sci***, 249, 37-52 (2017).
54. Z. Karvani and P. Chehrazi, "Antibacterial Activity of ZnO Nanoparticle on Gram-Positive and Gram-Negative Bacteria", ***Afr J Microbiol Res***, 5(12), 1368-1373 (2011).
55. J. Lakshmi, R. Sharath, M. Chandraprabha, E. Neelufar, A. Hazra and M. Patr, "Synthesis, Characterization and

Evaluation of Antimicrobial Activity of Zinc Oxide Nanoparticles", ***J Biochem Tech***, 3(5), 151-154 (2012).
56. C. Khatana, A. Kumar, M. Alruways, N. Khan, N. Thakur, D. Kumar and A. Kumari, "Antibacterial Potential of Zinc Oxide Nanoparticles Synthesized using *Aloe vera* (L.) Burm. f.: A Green Approach to Combat Drug Resistance", ***J Pure Appl Microbiol***, 15(4), 1907-1914 (2021).
57. K. Raghupathi, R. Koodali and A. Manna, "Size-Dependent Bacterial Growth Inhibition and Mechanism of Antibacterial Activity of Zinc Oxide Nanoparticles", ***Langmuir***, 27(7), 4020-4028 (2011).
58. N. Al-Hada, H. Kamari, C. Abdullah, A. Saion, A. Shaari, Z. Talib and K. Matori, "Down-Top Nanofabrication of Binary (CdO) (ZnO) Nanoparticles and Their Antibacterial Activity", ***Intern J Nanomed***, 12, 8309-8323 (2017).
59. A. Chauhan, R. Verma, S. Kumari, A. Sharma, P. Shandilya, X. Li, K. Batoo, A. Imran, S. Kulshrestha and R. Kumar, "Photocatalytic Dye Degradation and Antimicrobial Activities of Pure and Ag-Doped ZnO Using *Cannabis sativa* Leaf Extract", ***Sci Rep***, 10, 7881 (2020).
60. Y. Slavin, J. Asnis, U. Häfeli and H. Bach, "Metal Nanoparticles: Understanding The Mechanisms Behind Antibacterial Activity", ***J Nanobiotech***, 15, 65 (2017).
61. R. Brayner, R. Ferrari-Iliou, N. Brivois, S. Djediat, M. Benedetti and F. Fievet, "Toxicological Impact Studies Based on *Escherichia coli* Bacteria in Ultrafine ZnO Nanoparticles Colloidal Medium", ***Nano Lett***, 6(4), 866-870 (2006).
62. L. Zhang, Y. Jiang, Y. Ding, M. Povey and D. York, "Investigation Into The Antibacterial Behavior of Suspensions of ZnO Nanoparticles (ZnO Nanofluids)", ***J Nanopart Res***, 9, 479-489 (2007).
63. P. Espitia, N. Soares, J. Coimbra, N. Andrade, R. Cruz and E. Medeiros, "Zinc Oxide Nanoparticles: Synthesis, Antimicrobial Activity and Food Packaging Applications", ***Food Bioproc Tech***, 5, 1447-1464 (2012).
64. V. Shinde, D. Dalavi, S. Mali, C. Hong, J. Kim and P. Patil, "Surfactant Free Microwave Assisted Synthesis of ZnO Microspheres: Study of Their Antibacterial Activity", ***Appl Surf Sci***, 307, 495-502 (2014).
65. A. Sirelkhatim, S. Mahmud, A. Seeni, N. Kaus, L. Ann, S. Bakhori, H. Hasan and D. Mohamad, "Review on Zinc Oxide Nanoparticles: Antibacterial Activity and Toxicity Mechanism", ***Nano Micro Lett***, 7, 219-242 (2015).
66. B. Silva, M. Abuçafy, E. Manaia, J. Junior, B. Galdorfini, C. Andréo, R. Pietro and L. Chiavacci, "Relationship Between Structure and Antimicrobial Activity of Zinc Oxide Nanoparticles: An Overview", ***Inter J Nanomed***, 14, 9395-9410 (2019).
67. N. Padmavathy and R. Vijayaraghavan, "Enhanced Bioactivity of ZnO Nanoparticles—An Antimicrobial Study", ***Sci Tech Adv Mat***, 9(3), 035004 (2008).
68. P. Stoimenov, R. Klinger, G. Marchin and K. Klabunde, "Metal Oxide Nanoparticles as Bactericidal Agents", ***Langmuir***, 18(17), 6679-6686 (2002).
69. S. Gad El-Rab, A. Abo-Amer and A. Asiri, "Biogenic synthesis of ZnO nanoparticles and its potential use as antimicrobial agent against multidrug-resistant pathogens", ***Curr Microbiol***, 77(8), 1767-1779 (2020).

Bull. Pharm. Sci., Assiut University, Vol. 47, Issue 1, 2024, pp. 499-517.

نشرة العلوم الصيدلية
جامعة أسيوط

BULL. PHARM. SCI. Assiut Univ.

# التخليق الحيوي لجزيئات أكسيد الزنك النانوية باستخدام مستخلص أوراق الصبار وتأثيرهم المضاد للبكتيريا

**مجدي أبو غربية – جيهان سالم – جهاد العربي***

**قسم النبات والأحياء الدقيقة ، كلية العلوم ، جامعة سوهاج ، ٨٢٥٢٤ سوهاج ، مصر**

اكتسبت جزيئات أكسيد الزنك النانوية اهتمامًا كبيرًا كبديل علاجي واعد للمضادات الحيوية. في هذه الدراسة، تم إجراء التخليق الحيوي لجزيئات أكسيد الزنك النانوية باستخدام مستخلص أوراق الصبار بطريقة بسيطة للغاية. تم الكشف عن جزيئات أكسيد الزنك النانوية المُصنّعة حيويًا بواسطة مقياس الطيف الضوئي للأشعة فوق البنفسجية عند الطول الموجي ٣٨٣ نانومتر. أشار تحليل حيود الأشعة السينية إلى وجود تركيب سداسي لجسيمات أكسيد الزنك النانوية ذات متوسط حجم بلوري قدره ١٦.٧ نانومتر. أظهر المجهر الإلكتروني النافذ والماسح الشكل السداسي لجسيمات أكسيد الزنك النانوية بمتوسط حجم جسيم يبلغ ٢٠ نانومتر تقريبا. أظهر تحليل فورييه للأشعة تحت الحمراء التواجد المشترك للمركبات الفينولية في كلا من مستخلص أوراق الصبار وجزيئات أكسيد الزنك النانوية مما يشير إلى دورها الرئيسي في عملية الاختزال الحيوي. من وجهة نظرنا، فإن الظروف المثلى للتخليق الحيوي لجزيئات أكسيد الزنك النانوية ذات أحجام صغيرة تشمل تركيز نترات الزنك ٠.٠١-٠.٠٣ م، وتركيز مستخلص الصبار ٥٠٪، قيمة الاس الهيدروجيني= ٨، و٢٥-٤٠ درجة مئوية. تم التأكد من التأثير المضاد للبكتريا لجزيئات أكسيد الزنك النانوية ضد كلا من البكتريا سالبة الجرام وموجبة الجرام. تراوحت قيم أقل تركيز مانع لنمو البكتريا من ٢ إلى ٤.١ ملجم/مل ومن ٨.٢ إلى ١١ ملجم/مل لكلا من البكتيريا سالبة الجرام وموجبة الجرام على التوالي. علاوة على ذلك، أظهرت جزيئات أكسيد الزنك النانوية تأثيرًا مميتا للجراثيم ضد كل من العزلات البكتيرية سالبة الجرام وإيجابية الجرام التي تم اختبارها حيث تراوحت قيم أقل تركيز قاتل للبكتريا من ٢.١ إلى ٤.٧ ملجم/مل ومن ٨.٢ إلى ١١.٤ ملجم/مل لكلا من البكتيريا سالبة الجرام وموجبة الجرام على التوالي.